

High Gradient Magnetic Fields Generated in Events on the 230 kV Electric Power Transmission Infrastructure: Human Exposure Analysis and Risk

FABIAN RICARDO ROJAS¹, GERARDO GUERRA¹, SERGIO RIVERA²

¹Enlaza-GEB,
COLOMBIA

²Departamento de Ingeniería Eléctrica,
Universidad Nacional de Colombia SEDE Bogotá,
COLOMBIA

Abstract: - This work presents a process for analyzing human exposure to high-gradient magnetic fields based on protection models for patients undergoing magnetic resonance examinations developed by the International Commission on Non-Ionizing Radiation Protection (ICNIRP). A series of events presented in the electrical energy transmission infrastructure is taken, with typical currents and front times, a case of extreme failure is added, and results are presented. Subsequently, with a classic lightning signal, compliance with the exposure to this type of field in the right-of-way strip of a transmission line is verified and validated in the event of a hypothetical atmospheric discharge impact event. Finally, a simulation is implemented with space discretization techniques, establishing the signal resulting from the magnetic field generated as a function of time. The exposure is evaluated using the presented model. Only in one of the analysis cases was it found that the perception threshold is exceeded at distances less than 0.6 cm, virtually a situation in which the worker has contact with the down conductor. With the results obtained and the cases analyzed, it is concluded that failures of this type do not generate significant exposure to high-gradient magnetic fields and do not exceed the determined perception thresholds.

Key-Words: - Magnetic Field, Transmission Line, Fault Current, Lightning, High Voltage, Substation.

Received: April 28, 2024. Revised: September 9, 2024. Accepted: October 8, 2024. Published: November 13, 2024.

1 Introduction

The electric power transmission infrastructure fulfills a strategic function for our society, carrying electric power from generation centers to consumption centers. This network is frequently exposed to incidents in the operation of Substations (SE) and Transmission Lines (LT) caused by atmospheric discharges or transient voltage and/or current events, which originate the emission of electromagnetic fields of high amplitude and high gradient. These phenomena have been the subject of analysis and research that have allowed the establishment of strategies to characterize risk exposure, generating a knowledge base on the possible effects.

The exposure estimation methodologies that have provided the best results are those established within the recommendations and safety guidelines for magnetic resonance examinations. The characterization of the risk of being affected by this type of field is an essential element for the safe

operation and maintenance of the transmission infrastructure, but also for the general population in their areas of influence. With the growing concern and the evolution in the knowledge of the communities concerning the typical interactions of electromagnetic fields emitted by LT and SE with human health, concern has been generated regarding the exposure to high gradient fields in the vicinity of the easement strips, especially due to observations of atmospheric discharges that impact the infrastructure and failure modes that generate visually perceptible disruptions in isolation.

High gradient fields associated with industrial frequency are generally very limited by the designs and protection systems, so they do not present levels that can be perceived as dangerous. On the other hand, the fields that originated in atmospheric discharges are the highest gradient fields and those that have been the subject of the most in-depth analysis. Some investigations have reported that those phenomena that present characteristics of very

short front and tail times apparently would not have a harmful effect because they are much faster than the Chronaxie of tissue excitation. However, some research has also reported that slow atmospheric discharges with longer times of up to 200 μ s could generate a nerve stimulation effect. In addition, the electric and magnetic fields generated by overvoltages/overcurrents caused by events have front times that can be in the order of milliseconds, so they could be in the spectrum of nerve stimulation impulses and could have characteristics comparable to the limit determined for muscle stimulation. The possible effects associated with the magnetic field are of particular interest, which typically has no controls to mitigate the possible risk; on the other hand, the electric field has a specific control implemented through fixed or temporary grounding.

2 General Aspects of Exposure to Electric (EM) and Magnetic (EM) Field

The World Health Organization (WHO), in its role as the guiding and coordinating authority for health action in the United Nations system, plays a leading role in world health matters. With this focus, it commissioned the ICNIRP to prepare a set of recommendations and guidelines for the protection of people from non-ionizing radiation. As a result of this Commission's work, the conclusions on the scientific evidence related to the effects of NIR on health were published in 1998, which became a reference document for governmental, public, and private institutions responsible for the population's health, as well as for researchers in the field and the general public. These recommendations have been periodically updated and validated in documents published by ICNIRP from 1998 to the present, [1], [2].

Due to the diverse characteristics of the exposure, the impossibility of fully determining the causal effect, and the complexity associated with calculating the induced parameters, two types of values are considered for limiting EMF exposure. The exposure values associated with the basic restrictions are based on health effects that have been precisely established, and their values are given in induced physical quantities, making them difficult to measure in practice. To ensure protection against such effects, the corresponding values should never be exceeded, [3], [4], [5], [6].

The exposure values associated with the reference levels are obtained from the basic

restrictions, using mathematical models that relate the induced variables to more easily measurable physical parameters. In addition, they take into account the factors that can modify the exposure, in order to provide a direct comparison parameter. They are calculated for the condition of maximum coupling of the field with the exposed individual, frequency dependence, and dosimetric uncertainties, thus providing maximum protection, [4], [6]. If the measured values are higher than the reference levels, it does not necessarily imply that the basic constraints are being exceeded, but further analysis is essential to assess compliance with the basic constraints, [4], [5], [6].

ICNIRP recommendations are widely known for exposures to constant frequency fields or those whose spectral content can be decomposed into a reasonable number of components and specific constraints applied to each frequency, and then total weighting applied. High gradient fields with shapes far from sinusoidal and frequencies not characterizable with classical transforms must have different considerations for compliance verification in the framework of their exposure safety. Some models of lightning signals that can give rise to these fields can be found in [7].

Specifically for high gradient fields, ICNIRP has recommended three models for the evaluation of exposure to pulsed or complex signals, which can be consulted in detail in [2], [5], [6].

The first consists of converting the signal, generally rectangular, to an equivalent sinusoidal signal by adjusting the frequency of the resulting wave with the width of the original pulse. This method has weaknesses in complex waveforms since it ignores the signals superimposed on the equivalent main frequency, [5].

A second method consists of the spectral decomposition in frequency of the original signal and the unitary comparison of each of the amplitudes of the frequencies of the resulting spectrum, in relation to the limits determined for each frequency, weighting an overall exposure that adds one by one each exposure component. This method yields good results in periodic signals with several coherent cycles, however, it presents important weaknesses in non-periodic signals due to the convergence problem associated with the signal sampling and the low-frequency components resulting from using time-frequency transforms in truncated signals, [2], [5]. Filtering solutions have been proposed, however, for high gradient pulsed signals or narrow band sinusoidal bursts, they can artificially hide or reduce the exposure associated

with peak values that exceed the RMS values typically present in this type of signal, [2], [5].

A third approach is based on evaluating the exposure using dB/dt peak weighting of the signal and then calculating the induced current density using a constant of proportionality of the electrical conductivity of the tissue and the effective radius of the current loop, [8], [9]. This approach seeks to better approximate the characteristics of the waveforms and the nature of the biological interactions, [5], [6]. This approach presents weaknesses in the evaluation of high gradient fields because the proportionality constants for the calculation of induced current are theoretically derived from calculations for induced currents in the head originating in sinusoidal signals, which makes them overly conservative for high gradient fields, [2], [8].

The exposure and compliance estimation models used in the present work have been reviewed and published previously and present a good result for the characterization of the magnetic field with this type of characteristics, [2], [10], [11]. This one has remarkable advantages in its accuracy because they are derived from exposure thresholds in Magnetic Resonance Imaging (MRI) examinations [9], therefore, the way of development is based much more extensively on clinical trials and real exposure, measuring physical variables on cohorts of patients and volunteers, with this approach the biological constants are more accurate and the thresholds much more adjusted to the real measured exposure, without neglecting the precautionary principle, [10]. Moreover, because of the type of signal used in this type of examination, broader similarities with pulsed high-gradient signals are observed, [11].

3 High Gradient Magnetic Field Assessment Exposure Model

Initial evaluation models can be found in [2] and [8], but in the search for a complementary methodology, it is found that the lightning current signal and its associated magnetic field gradient have some similarities with the signals used medically for MRI. Taking advantage of this similarity, it is proposed to use the methodology to assess the safety of patients against the magnetic field emissions used in this type of examination and associate it to the signal of interest. Accordingly, we take as a reference what is proposed in [9], where an evaluation of the average perception threshold is proposed from the following expression:

$$\frac{dB}{dt} = 20 \left(1 + \frac{0.36}{\tau} \right) [T/s] \quad (1)$$

Where τ is the effective stimulus duration in [ms]. The effective stimulus duration is the duration of the monotonically increasing or decreasing gradient period [9].

It is been established in [9] that the cardiac stimulation threshold is well above the intolerable stimulation threshold for high gradient signals. Furthermore, the lowest percentile for intolerable stimulation is 20% above the average threshold for peripheral nerve stimulation. In that sense, the interest now is to establish whether the nervous stimulation threshold and the intolerable stimulation threshold are exceeded with an exposure such as the one studied.

For this objective, we analyze the academic and scientific references taken by ICNIRP [9] for the issuance of its recommendations within the framework of patient protection during MRI examinations. The basic equation of magnetic field gradient stimulation is presented in [10] and is defined as:

$$\frac{dB}{dt} = b \left(1 + \frac{c}{d} \right) [T/s] \quad (2)$$

Where b is the Rheobase, the asymptotic dB/dt for long-duration pulses, c is the Chronaxie, the pulse duration at which the dB/dt is twice the Rheobase and d is the pulse duration [10].

The population average has a perception threshold with values of $b=14.91$ [T/s] and $c=365$ [μ s] [10]. Significant contractions in the thoracic skeletal muscles were observed for magnetic field gradients approximately 50% higher than those associated with the perception threshold [10]. A dB/dt intensity of approximately twice the perception threshold was found to be intolerable [10]. Using these factors, the graphs of gradient intensity and effective stimulus duration are constructed, for the three thresholds of interest: perception threshold, muscular stimulation threshold, and intolerable stimulation threshold.

4 Failure and Exposure Analysis for Substations

As stated in previous sections, this work is motivated by analyzing two events that occurred in the electrical power transmission infrastructure in Colombia and Brazil, respectively. Both events occurred during asset operation and maintenance activities. In the first case, power equipment maintenance activities were performed on a 230 kV

line bay (BL). The associated transmission line (LT) has a double circuit, so BL1 was being worked on while BL2 remained in service. Physically, both line bays are arranged next to each other within the physical topology of a substation with a double busbar configuration with an interconnector. The conditions of the work to be performed required the opening and grounding of the LT at both ends of the line. During the execution of the activities, a ground current discharge occurred through the temporary grounding arrangements provided to protect the work area of the intervened BL. This condition forced the temporary suspension of the activity and the taking of additional actions to preserve the safety of the work teams participating in the maintenance. Following the Root Cause Analysis (RCA), it was established that a contact occurred between one of the phases of the in-service circuit and one of the phases of the maintenance circuit at a specific point on the LT. This situation gave rise to the incident and originated in atypical wind conditions in a geographical area within the LT corridor.

The second case also occurred during the maintenance of electrical equipment for substations on a 230 kV BL. The LT has a double circuit, so BL1 was disconnected while BL2 remained in service. Physically, both line bays are arranged side by side within the physical topology of a substation with a double bus configuration. The conditions of the work to be carried out required the opening and grounding of the LT at both ends of the line. During the execution of the activities, tests had to be carried out on the grounding switch. Due to loss of situational awareness and deviations in the execution of the maintenance procedure, the grounding switch of the energized bay (BL2) was closed, which generated a free ground fault that was evacuated by the solid ground connection of the disconnecter. After the event, the activity was temporarily suspended, and actions were taken according to the security incident procedure, evaluating the contingency and taking action to regain situational awareness and ensure operating conditions. A Root Cause Analysis (RCA) was subsequently developed.

Taking the described incidents as a reference, and in the search for more and more exhaustive analyses to guarantee the safety of the electrical industry personnel, and in general of any person close to high voltage infrastructures, the evaluation of the exposure to high gradient magnetic fields originated by the fault currents of different fault events is proposed. This evaluation is relevant and totally necessary to complement the widely

documented analyses (in the electrical industry literature) on exposure to industrial frequency electric fields or faults, which have specific control measures, such as the adequate design of grounding systems with the respective control and monitoring of step and contact voltages, and which are required in the technical regulations and standards applicable to the power transmission sector in Colombia and the world. On the other hand, exposure to high-gradient magnetic fields is an aspect that has not been extensively characterized and documented. In the framework of the precautionary principle, it is necessary to carry out analyses such as those proposed.

Figure 1 presents a schematic context of exposure to a high gradient magnetic field caused by a fault current flowing through the conductor of a temporary grounding equipment (TGE) while a worker performs activities on adjacent equipment at a short distance. This model assimilates to the operating condition of the first event described. The fault current, generated by the contact between the phases of circuit 1 and circuit 2 in the LT trace, flows through the conductor of the de-energized circuit to the SE. Due to the working conditions, the surge arresters are disconnected from their down conductors, and a (TGE) is connected between the temple and the grounding system connection of the SE, in the lattice at the base of the equipment. Under this operating scenario, the fault current flows directly to the ground through the (TGE) causing a high-gradient magnetic field in the area near the conductor. This current generates a magnetic field of similar waveform, which materializes the exposure of workers in the vicinity of the down conductor. This context is the one chosen for the following calculations and estimations, since it presents a higher exposure than the one generated in event two, due to the fact that in the latter the distance to the energized bay is wider because no work was being carried out there.

Thus, as indicated in the previous paragraphs and taking into account what was established in [8], [9] and [11], a high-gradient magnetic field could result in an induced current with acute harmful effects on the human body. Therefore, it would be plausible that a gradient of a fault current in the Transmission System can generate a field gradient that generates some interaction. Then, the fault current gradient will be calculated to analyze whether any overshoot of perception thresholds, muscle stimulation, or intolerable stimulation is possible.

To calculate the current gradient, an approximation of the upward ramp of the signal is

made, taking into account the condition of its monotonic increase to an almost linear characteristic. This approximation represents an error of less than 10% in signals up to twice as fast as a lightning current, in accordance with what is established in [2], so this approximation will not generate a marked uncertainty in the results.

With the current gradient, we now turn to Ampère's law, which allows us to calculate the magnetic field (B) caused by a time-varying current (I). It is necessary to take into account that this approach has some limitations associated with the finite length of the conductor that clears the fault current, the effect of field reflections generated by the equipment and supports adjacent to the grounding conductor, and the contributions of the fault currents that circulate through the earth. Assuming these conditions, the typical expression is used to calculate the magnetic field generated by an infinite streamline, and expressing it in terms of its time derivative, we obtain:

$$B = \frac{\mu_0 I}{2\pi \cdot d} \rightarrow \frac{dB}{dt} = \frac{\mu_0}{2\pi \cdot d} \frac{di}{dt} \quad (3)$$

With d representing the distance in meters to the infinite current line, B is the magnetic field, I am the current, and μ_0 It is the vacuum permeability.

Once the expression that relates the derivative of current with the derivative of the magnetic field is established, four fault events of the 230 kV transmission system cleared by the relay-switch assembly are selected to calculate the exposure they could generate under conditions like those described.

Figure 2 presents the oscillographs of the currents of the three phases of four selected events. From left to right the faults are presented in phase C, phase A, phase B, and phase B, respectively. With a descending order of the signals for the phases, top A, middle B, and bottom C. Schematically two vertical lines and two vertical arrows in blue and yellow are used to highlight the beginning of the smoothed current ramp and the end of the smoothed current ramp. Which are used to calculate the amplitude and the monotonic rise time, in the faulted phase that has the highest current amplitude, and which is where the sharpest gradient occurs.

Table 1 record the current and monotonic time parameters of each fault for the calculation of current derivatives. To have an even more conservative evaluation, the inclusion of an assumed critical event with the most drastic fault conditions is determined, a current of 40 kA with a time of 8.3 ms (valley-peak time of the industrial frequency),

this event seeks a calculation under the worst fault conditions. It is at the limit of supportability of some of the equipment installed in the 230 kV substations.

Figure 3 (Appendix) presents the results of calculating the magnetic field derivatives in a homogeneous monotonic time for all the faults, in contrast to the thresholds of perception, muscular stimulation, and intolerable stimulation. The distance scale on the x-axis is in cm and allows observation that from 0.75 cm, none of the faults would generate an overshoot of any of the thresholds. The 40 kA critical fault can exceed the perception threshold only at distances of less than 0.6 cm from the source; an overrun of the muscle stimulation threshold occurs at a distance of 1 mm, i.e., virtually when the worker is in contact with the conductive element through which the fault current flows. This situation is extremely remote, and if it were to materialize, the risks associated with the electric field or its thermal effects would be of greater concern.

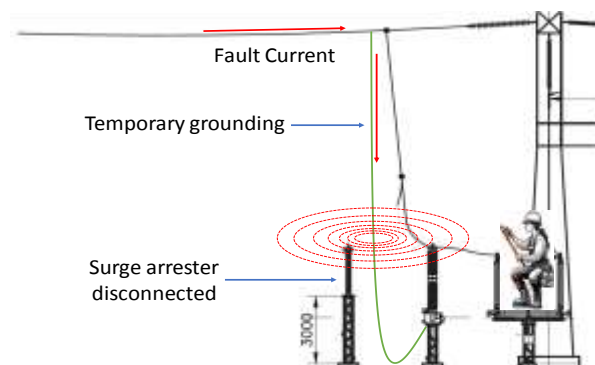


Fig. 1: Schematic model of fault current flow through grounding equipment while working on adjacent equipment

The analysis is performed with the ramp of the highest current gradient; the analysis with successive ramps in the framework of the signal damping yields lower results than those presented. According to the results obtained in events where the exposed worker is more than 0.75 cm from the current source, no effect would be expected.

5 Proposed Analysis: Lightning Signal Model

Works such as the one presented in [8] and [11] have shown possible acute effects at distances less than 30 cm from cables carrying lightning fault currents. Based on these analyses, a calculation of possible exposures to high gradient fields in the

easement strips in certain cases of lightning strikes on TL infrastructure is proposed.

Table 1. Fault currents and times for calculating current gradients

Event Class	Fault current [kA]	Monotonic Time [ms]	Substation voltage
Event 1	1.89	8.3	230 kV
Event 2	2.65	8.3	230 kV
Event 3	4.38	8.1	230 kV
Event 4	10.7	8.5	230 kV
Assumed critical event	40	8.3	230

For this purpose, a typical lightning signal is selected, and an analysis similar to the one presented for SE is performed.

A typical time domain lightning signal is proposed for the analysis, as suggested in [7], and is presented in equation 4.

$$i = \frac{I}{k} * \frac{\left(\frac{t}{\tau_1}\right)^5}{1 + \left(\frac{t}{\tau_1}\right)^5} * \exp\left(\frac{-t}{\tau_2}\right) \quad (4)$$

Where i is the current signal, I is the peak current in [kA], k is the correction factor for the peak current, t time in [μ s], τ_1 the front time constant, and τ_2 decay time constant

The peak current parameters and characteristic times of the lightning signal are established as a reference to what was stated in [7] to determine probabilistic magnitudes of the parameters 95%, 50%, 5%, and <1%—the Table 2 presents the parameters of the selected signals, and

Fig. 4 (Appendix) shows the resulting signals in the time domain.

Table 2. Lightning signal parameters

I [kA]	k	t1	t2	Probabilistic magnitude
24	0.981	0.324	70.45	95%
45	0.981	0.324	70.45	50%
85	0.981	0.324	70.45	5%
200	0.981	0.324	70.45	<1%

5.1 Event Analysis for a Lightning Strike on an LT

The analysis for TL is based on the assumption of a lightning strike on the power cable or guard with peak current values between 24 and 200 kA, assuming that at that exact moment, there is a

worker in the easement strip. Under typical conditions the current flows in both directions away from the point of impact, with amplitudes and wavefronts determined by the impedances of the cable, towers, grounding, and their interactions. These reduce the gradients and maximum amplitudes of each of the wavefronts. To perform conservative calculations, the assumption is made that all the lightning current flows in a single direction, and attenuations of the medium and impedances are discarded. Thus, the maximum amplitude and maximum gradient scenario is obtained, which is desirable in this type of exposure calculation. The Fig. shows the impact scenario and the signals used for the proposed calculation.

Fig. (Appendix) shows the results for a fast front time with different amplitudes, in contrast to the thresholds for perception, muscle stimulation, and intolerable stimulation for that gradient time. It can be seen that only with the 200-kA signal at a distance of 50 cm the perception threshold is exceeded, which demonstrates that even in a scenario of very high and remotely probable current, any worker in the easement strip would not have effects associated with exposure to high gradient magnetic fields.

5.2 Discretization Space Simulation

Although the analytical results clearly show that there is no evident effect on the exposure of the analyzed cases, to finalize this study, a simulation is implemented using spatial discretization techniques software with a lightning-type signal, which was the one that showed higher derivatives and higher exposure incidence in the previous calculations.

The software used is CST Studio Suite, which implements the Finite Integration Technique (FIT) and the Transmission Line Method (TLM), which allows properly simulating of the return channel and its associated fields, as well as the coupling effects. This software has a presence of several decades in the market of physical and electromagnetic simulations, is widely validated, and is used by multiple engineering companies worldwide. This software allows simulation directly in the time domain, improving some of the results of other software that uses frequency domain techniques and use back transforms to adjust the results in time, [12].

The spatial domain is 20m x 20m x 20m, with PML (Perfectly Matched Layer) boundaries that generate a boundary condition with no absorptions or reflections in the signals. A concrete block of 10m x 10m x 5m is included, and a downspout of radius 0.02m and 5.2m high penetrates the block 0.2

m, as shown in Fig. (Appendix), left side. The excitation signal is a classical double ramp signal with an amplitude of 200 kA, as shown in Figure 7 (Appendix) on the right side. The simulation occurs in the time domain between 0 and 100 μ s.

Fig. and Figure 8 (Appendix) presents the simulation results; on the left, the magnetic field distribution around the down conductor, a field concentration is observed in the vicinity of the excitation source. On the right, the magnetic field signal is in [A/m]. The results show that for the maximum gradient interval, the thresholds of perception, muscle stimulation, or intolerable stimulation are not exceeded. There is a significant deviation in the simulation results Vs. the analytical calculation because the exposure calculated in previous sections has maximum coupling factors and is markedly conservative; in addition, they are made with an infinitely long conductor approximation, [13]. On the other hand, the simulations are theoretically more accurate and consider the presence of the concrete block.

Additional simulations with the presence of a support structure or additional equipment to show the field distortion would be desirable. However, the software used is in a student test license and has extensive restrictions for meshing, which prevented the realization of more complex simulations. The student version allows a maximum of 100,000 mesh cells. According to the determined simulation space the maximum simulation accuracy is for a discretization of $2 * 10^{-4} \text{ m}^3$.

Nevertheless, the results obtained clearly show that the levels of exposure to high gradient magnetic field are marginal for the models analyzed.

6 Conclusion

Verification and validation of the exposure of high gradient magnetic fields originating from fault currents are necessary because, under certain conditions, it has the possibility of exceeding the perception, muscle stimulation, or intolerable stimulation thresholds. One of the best methods that has been documented is the use of assessment methodologies for patient safety during MRI examinations.

Results obtained from theoretical analysis and computational simulations show mismatches due to the approximate characteristics of the theoretical equations since their models do not take into account environmental elements, such as the ground or adjacent elements. However, analytical models are a valuable tool for initial verifications, with great ease of application and usable results.

Analysis developed for power system failures with peak currents of up to 40 kA and front times of 8.3 ms show that the perception threshold is only exceeded at distances less than 0.6 cm from the source. The stimulation threshold is only exceeded in very remote conditions in which the worker is virtually touching the downspout conductor; in this scenario, risks associated with the electric field or thermal stress may be more acute.

Results obtained from the analysis with a rapid atmospheric discharge of 200 kA amplitude show that none of the thresholds of interest are exceeded in the easement strip. Exceeding the perception threshold only occurs 50 cm from the conductor, a scenario only possible for a worker who is passing by the transmission line conductor just at the moment when the lightning strike occurs.

In this way, this paper stood out for its analysis of human exposure to high-gradient magnetic fields originating from events on the 230 kV electric power transmission infrastructure. It presents a range of scenarios, including typical events and extreme failures, and verifies compliance with exposure thresholds. Additionally, the inclusion of a lightning signal model added depth to the analysis, showing the potential impact of atmospheric discharges on exposure levels. Thus, this paper provided valuable insights into a critical aspect of electrical infrastructure safety, shedding light on potential risks and offering a basis for further research and safety measures.

Declaration of Generative AI and AI-assisted Technologies in the Writing Process

During the preparation of this work the authors used CLAUDE in order to study the state of the art and the missing development in order to give a new approach our proposal. After using this tool/service, the authors reviewed and edited the content as needed and take full responsibility for the content of the publication.

References:

- [1] International Electrotechnical Commission, "IEC 62305 - Protection against Lightning," IEC, Geneva, Switzerland, 2010, [Online]. <https://webstore.iec.ch/publication/60559> (Accessed Date: October 14, 2024).
- [2] A. K. Gupta, N. G. Prakash, and T. R. Viswanath, "Human Exposure to Electromagnetic Fields: A Review of the Current Knowledge," *IEEE Access*, vol. 9, pp.

- 155653–155663, Nov. 2021. doi: [10.1109/ACCESS.2021.3115824](https://doi.org/10.1109/ACCESS.2021.3115824).
- [3] C. A. M. Pavan and M. J. S. Ferreira, "Effects of Electromagnetic Fields on Human Health," in *Human Health Effects of Electromagnetic Fields*, A. S. A. Al-Ali, Ed., International Conference on Electromagnetic Fields, 2021, pp. 1-15. doi: [10.1007/978-3-030-51938-2_1](https://doi.org/10.1007/978-3-030-51938-2_1).
- [4] ICNIRP, "Guidelines for Limiting Exposure to Time-Varying Electric, Magnetic, and Electromagnetic Fields (up to 300 GHz)," *Health Physics*, vol. 74, no. 4, pp. 494–521, Apr. 1998. doi: [10.1097/00004032-199804000-00023](https://doi.org/10.1097/00004032-199804000-00023).
- [5] ICNIRP, "Guidance On Determining Compliance Of Exposure To Pulsed And Complex Non-Sinusoidal Waveforms Below 100 kHz With ICNIRP Guidelines," *Health Physics*, vol. 85, no. 4, pp. 383–387, Oct. 2003. doi: [10.1097/01.HP.0000072980.35049.4F](https://doi.org/10.1097/01.HP.0000072980.35049.4F).
- [6] ICNIRP, "Guidelines for Limiting Exposure to Time-Varying Electric and Magnetic Fields (1 Hz to 100 kHz)," *Health Physics*, vol. 99, no. 6, pp. 818–836, Dec. 2010. doi: [10.1097/HP.0b013e3181f06c86](https://doi.org/10.1097/HP.0b013e3181f06c86).
- [7] National Fire Protection Association, "NFPA 780: Standard for the Installation of Lightning Protection Systems," NFPA, Quincy, MA, USA, 2017, [Online]. <https://www.nfpa.org/codes-and-standards/all-codes-and-standards/list-of-codes-and-standards> (Accessed Date: October 14, 2024).
- [8] Z. A. Tamus, B. Novak, S. V. Szabo, I. Kiss, and I. Berta, "Can the Near Field of Lightning Impulse in Down Conductors Cause Harmful Health Effects?" in *30th International Conference on Lightning Protection (ICLP)*, Cagliari, Italy, 2010, pp. 1–4. doi: [10.1109/ICLP.2010.7845793](https://doi.org/10.1109/ICLP.2010.7845793).
- [9] ICNIRP, "Medical Magnetic Resonance (MR) Procedures: Protection of Patients," *Health Physics*, vol. 87, no. 2, pp. 197–216, Aug. 2004, [Online]. <http://www.ncbi.nlm.nih.gov/pubmed/15257220> (Accessed Date: October 14, 2024).
- [10] F. G. Shellock, *Magnetic Resonance Procedures: Health Effects and Safety*, Boca Raton, FL: CRC Press, 2000. doi: [10.1201/9781420040004](https://doi.org/10.1201/9781420040004).
- [11] International Electrotechnical Commission, "IEC 62305 - Protection against Lightning," IEC, Geneva, Switzerland, 2010, [Online]. <https://webstore.iec.ch/publication/60559> (Accessed Date: October 14, 2024).
- [12] R. P. O. de Araújo, M. Z. Lima, and A. A. Guiot, "Assessment of Lightning Protection System Design Based on the IEC 62305-3 Standard," *IEEE Latin America Transactions*, vol. 14, no. 4, pp. 1778–1783, Apr. 2016. doi: [10.1109/TLA.2016.7452461](https://doi.org/10.1109/TLA.2016.7452461).
- [13] C. Baron, A. S. Al-Sumaiti, and S. Rivera, "Impact of Energy Storage Useful Life on Intelligent Microgrid Scheduling," *Energies*, vol. 13, no. 4, p. 957, 2020. doi: [10.3390/en13040957](https://doi.org/10.3390/en13040957).

Contribution of Individual Authors to the Creation of a Scientific Article (Ghostwriting Policy)

Conceptualization G.G., F.R., S.R.; methodology, software, validation, formal analysis G.G., F.R., S.R.; investigation, G.G., F.R.; writing—original draft preparation, G.G., F.R.; writing—review and editing, G.G., F.R., S.R. The authors have read and agreed to the published version of the manuscript.

Sources of Funding for Research Presented in a Scientific Article or Scientific Article Itself

No funding was received for conducting this study.

Conflict of Interest

The authors have no conflicts of interest to declare.

Creative Commons Attribution License 4.0 (Attribution 4.0 International, CC BY 4.0)

This article is published under the terms of the Creative Commons Attribution License 4.0 https://creativecommons.org/licenses/by/4.0/deed.en_US

APPENDIX

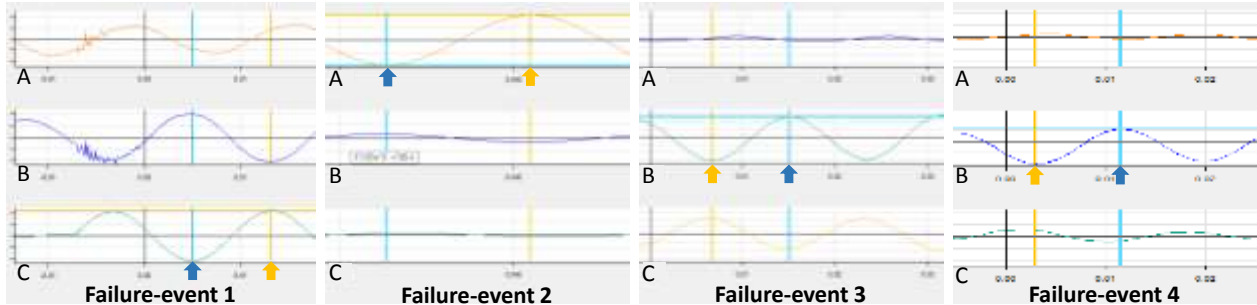


Fig. 2: Fault oscillographs. Failure 1 Phase C, failure 2 Phase A, failure 3 Phase B, failure 4 Phase B. Phases A, B, and C are assigned downstream. Monotonic time and gradient calculated in the middle of the indicator's blue and yellow cursors

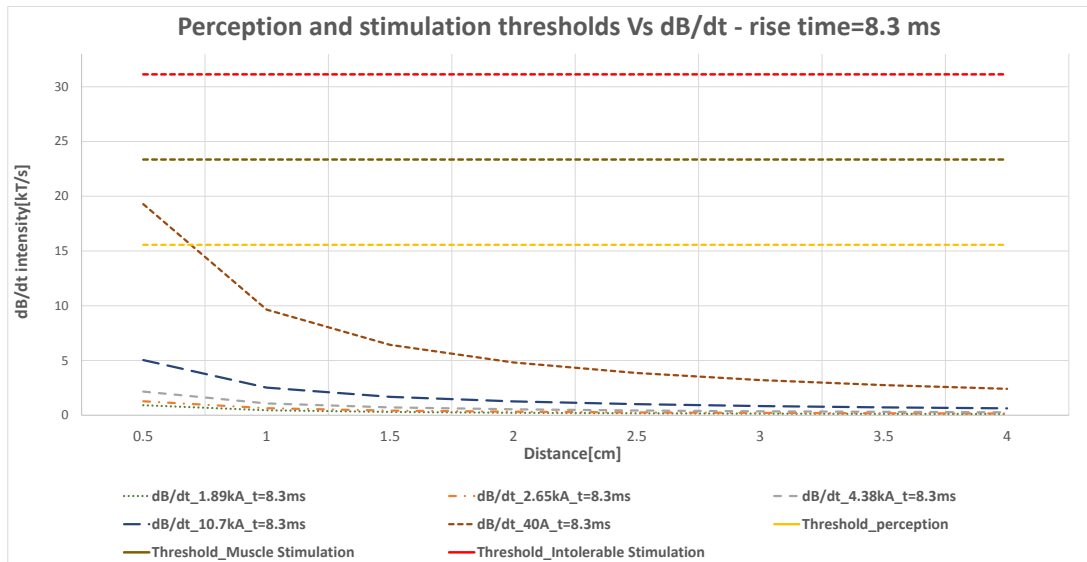


Fig. 3: Results of the calculation of the magnetic field derivatives in a homogeneous monotonic time for all faults, in contrast to the thresholds of perception, muscular stimulation, and intolerable stimulation

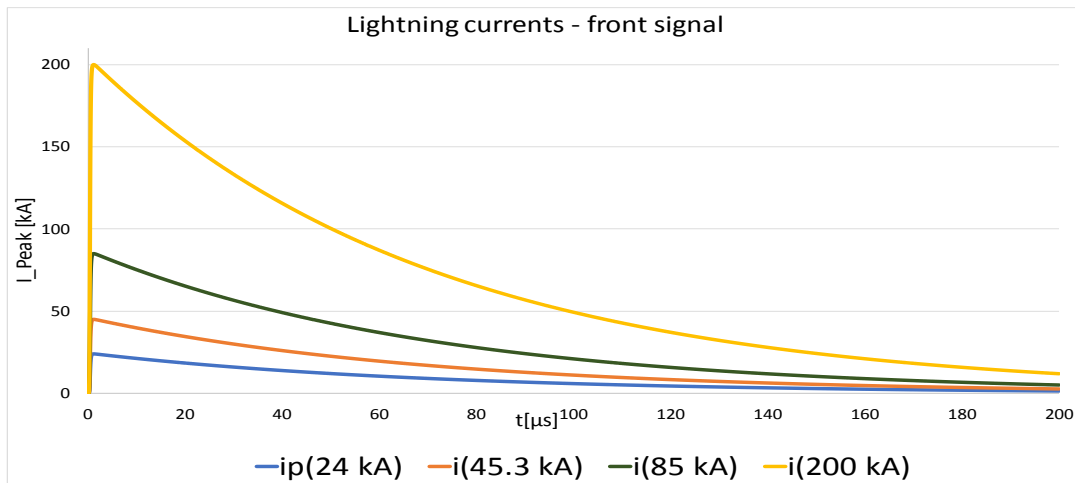


Fig. 4: Lightning signals in the time domain

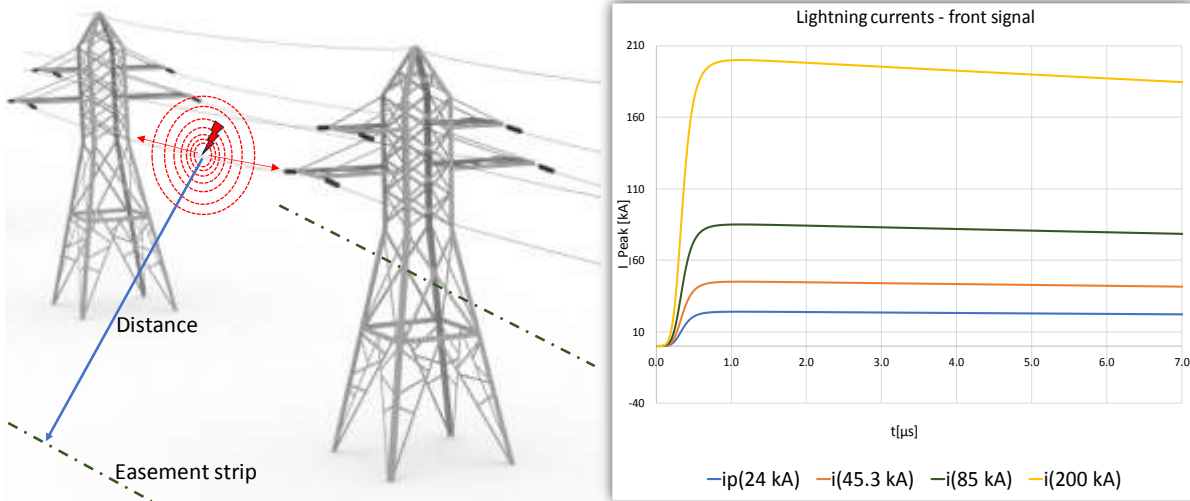


Fig. 5: On the left diagram is the lightning strike and field emission in the strip. The right fronts of ray signals were determined for the calculations

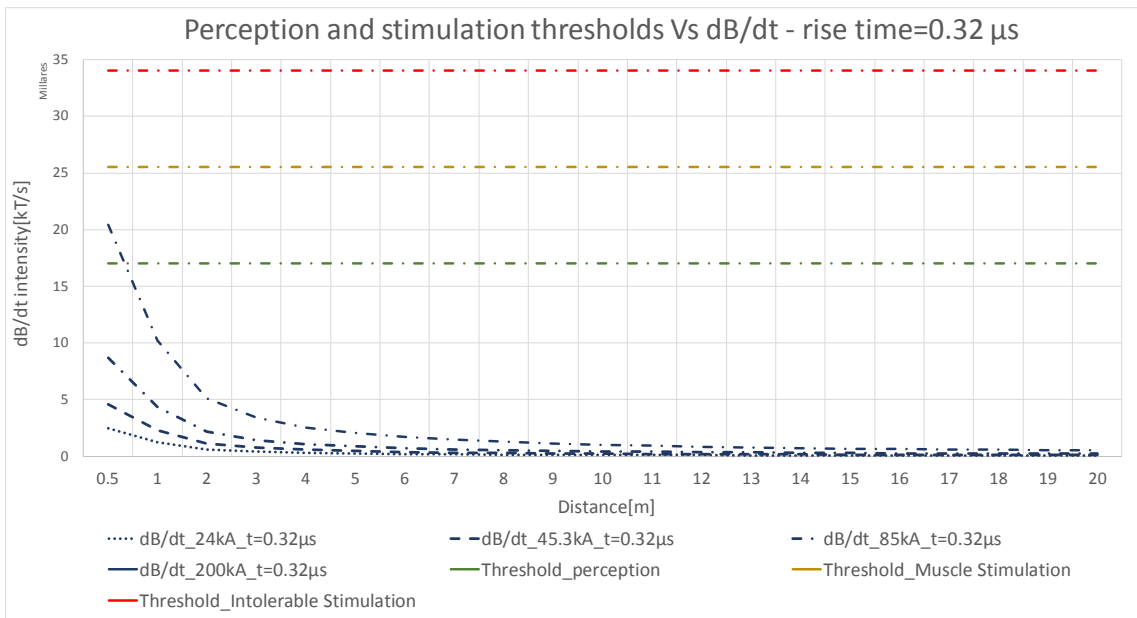


Fig. 6: Results of the magnetic field derivatives for fast front time and their comparison with the thresholds of perception, stimulation, and intolerable stimulation

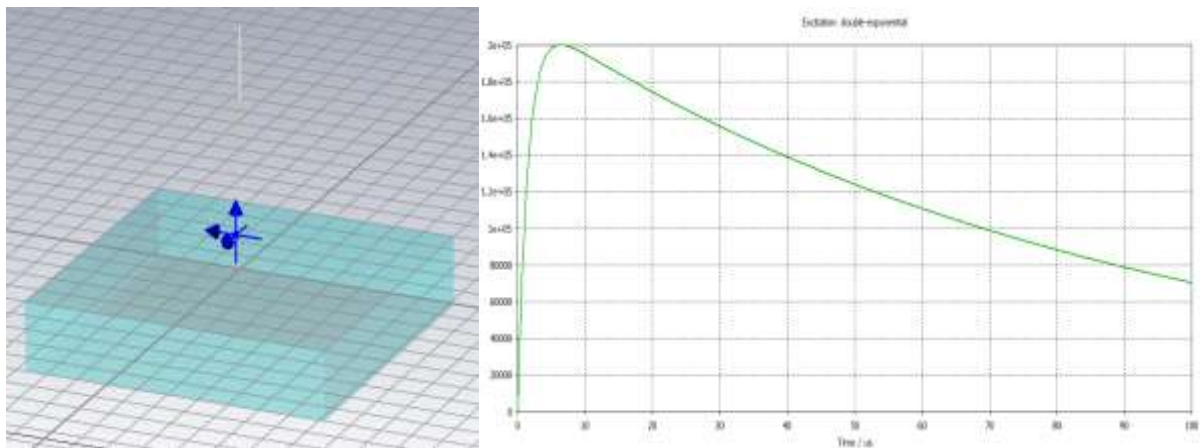


Fig. 7: Left simulation model with concrete block and down conductor. Right model excitation function

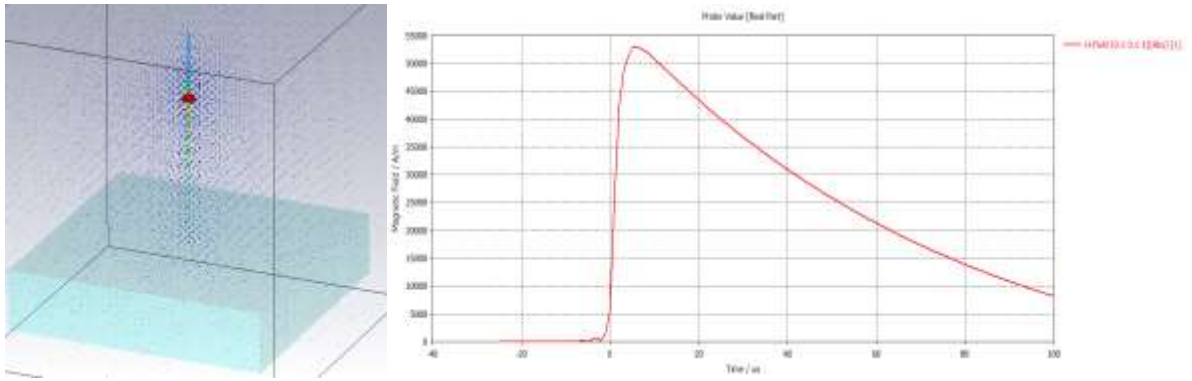


Fig.8: Simulation results, left magnetic field distribution in space. Right absolute magnetic field signal in [A/m] at test point 14 cm from the down conductor